ZIBELINE INTERNATIONAL™ PUBLISHING

ISSN: 2682-7786 (Online)
CODEN: BDAIDR

Big Data In Agriculture (BDA)

DOI: http://doi.org/10.26480/bda.01.2021.01.05

RESEARCH ARTICLE

MAPPING SPATIAL DISTRIBUTION OF MAIN SEASON RICE FIELDS IN EASTERN NEPAL USING MULTI-TEMPORAL LANDSAT 8 IMAGES

Samita Thapa*, Janma Jaya Gairhe

Institute of Agriculture and Animal Science, Tribhuvan University, Nepal.
****Corresponding author email: samitathapa38@gmail.com***

ARTICLE DETAILS

Article History:

Received 03 September 2020
Accepted 04 October 2020
Available online 19 October 2020

ABSTRACT

Mapping rice area can be beneficial for change detection, irrigation management, climate change impact and vegetation protection and restoration programs. Remote sensing has provided a vantage means of mapping rice area. The unique physical characteristics of rice plants is that it is grown in flooded soil, which significantly affect the spectral reflectance from the rice fields. After a period of two months, the dense rice canopy cover replaces the flooded soil. This dynamic of the rice field is captured with the help of vegetation indices and are used to identify rice fields. Multi-spectral and multi-temporal data Landsat 8 data is used in the study. An algorithm that uses Normalized difference vegetation index (NDVI) and Land-surface Water Index (LSWI) derived from Landsat 16-days 30-meter data was used to differentiate paddy field from other areas. It works on the basis of sensitivity of LSWI for surface moisture and NDVI for vegetation content. This algorithm was used to detect rice fields in twelve local levels in Sunsari and Morang districts of Nepal. The results were validated using 0.44m resolution digital globe satellite imagery with 79 well-distributed control points. The overall accuracy of the method was found to be 79.746%.

KEYWORDS

Paddy, NDVI, Food Security, Remote Sensing, LSWI, GIS.

1. INTRODUCTION

Rice ranks first amongst the cereal crops in terms of area and production in Nepal. It accounts about 40% of the total caloric intake. Contributing about 7% in the GDP of Nepal, it plays a huge role in food security of the country. Despite its importance, much of the rice cultivated are rain-fed. Main season rice is transplanted after the onset of monsoon between June to August and is harvested between September to November (MoAD, 2015). Nepal was an exporter of rice until the early 1980s. However, due to population growth and increased consumption of rice, it is slowly turning to be an importer. Mapping rice area can be beneficial for change detection, irrigation management, climate change impact and vegetation protection and restoration programs (MoAD, 2015).

Rice area determination is done by collecting information from individual farmers through surveys. This method takes a long time, which includes extensive field visits. This method is very tedious, time consuming, labour-intensive, expensive and not very accurate. It would be beneficial to gain information about the rice area more quickly to make better judgement about the rice sufficiency and import status (Mosleh et al., 2015). Application of remote sensing for monitoring land and surface change dynamics is evident. It has been extensively used for land use and land cover changes (Chhetri, 2017; Aburas et al., 2015; Meng et al., 2020; Ishtiaque et al., 2017; Rahman, 2016). Recently, remote sensing is being used for mapping rice field. It has provided a vantage means of mapping rice areas.

The unique physical characteristics of rice plants is that it is grown in flooded soil. The presence of water in the fields significantly affect the spectral reflectance from the rice fields. Temporal changes in the indices like Normalized difference vegetation index (NDVI), Enhanced Vegetation Index (EVI) and Land-surface Water Index (LSWI) can be used to detect the paddy fields. Different wavelengths of the solar radiation are absorbed differently by green vegetation. The absorption becomes maximum at 0.69 µm (Red band) due to chlorophyll while it becomes minimum at 0.85 µm (Near Infra-red band(NIR)) due to leaf cellular structure (Myneni et al., 1995). This absorption difference is used to indicate vegetation health. A healthy green vegetation reflects a huge amount of NIR but less in the red region. Similarly, short wave infra-red radiation (SWIR) is very sensitive to water content and is used for water monitoring (Joshi and Dongol, 2018). LSWI is sensitive to leaf water content and soil moisture changes (Chandrasekar et al., 2010).

Soil brightness affects vegetation indices in partially vegetated canopies. However, the flooded condition in the paddy field, soil brightness has little to no influence in the spectral indices. Leaf Area Index (LAI) in a paddy field is an important biophysical parameter that correlates with the crop growth, biomass and productivity. The spectral indices were highly correlated with LAI. Previous studies have proved that there is a strong linear relationship between NDVI and LAI in a paddy field (Xiao et al., 2002). Meanwhile, LSWI can be used to detect vegetation moisture and soil water content(Sari et al., 2010). A group researcher have used time series MODIS data to monitor rice phenology using EVI and LWSI (Sari et al., 2010). In other study, they used both EVI and NDVI in combination with LSWI to map paddy in Southern China (Xiao et al., 2005). In other hand, researchers have mapped major crops of chitwan district using sentinel data (Yadav et al., 2017). Similarly, mapped rice using sentinel-1 data in the cloud prone area of Bangladesh and Northeast India using cloud free Synthetic Aperture Radar (SAR) data from sentinel-1 satellite and random

Quick Response Code	Access this article online	
	Website: www.bigdatainagriculture.com	DOI: 10.26480/bda.01.2021.01.05

Cite The Article: Samita Thapa, Janma Jaya Gairhe(2021),Mapping Spatial Distribution Of Main Season Rice Fields In Eastern Nepal Using Multi-Temporal Landsat 8 Images. *Big Data In Agriculture, 3(1): 01-05.*

forest classifier (Singha et al., 2019). Landsat 8 data includes 11 bands in visible, near infrared, short wave infrared, panchromatic and thermal infrared region (Emara et al., 2018).

Table 1: Landsat 8 Bands Designations

Landsat 8	Bands	Wavelength (micrometres)	Resolution (meters)
Operational Land Imager (OLI) and Thermal Infrared Sensor (TIRS)	Band 1 – Coastal/aerosol	0.43 - 0.45	30
	Band 2 – Blue	0.45 - 0.51	30
	Band 3 – Green	0.53 - 0.59	30
	Band 4 – Red	0.64 - 0.67	30
	Band 5 – Near Infrared (NIR)	0.85 - 0.88	30
	Band 6 – Shortwave Infrared (SWIR) 1	1.57 - 1.65	30
	Band 7 - Shortwave Infrared (SWIR) 2	2.11 - 2.29	30
	Band 8 – Panchromatic	0.50 - 0.68	15
	Band 9 – Cirrus	1.36 - 1.38	30
	Band 10 – Thermal Infrared (TIRS) 1	10.60 - 11.19	100
	Band 11 - Thermal Infrared (TIRS) 2	11.50 - 12.51	100

The objective of this study is to estimate the potential of algorithm for identifying inundation and rice fields in terai region of Nepal using high resolution Landsat 8 images. Previously, other researcher has mapped temporal changes in rice area in Nepal with 500 m resolution MODIS data using unsupervised classification method (Gumma et al., 2011). However, in this study, algorithm for mapping rice area specifically were used. Daily MODIS data have high temporal resolution, but their low spatial resolution makes them unable to capture small field size and mixed agricultural landscape, especially in case of Nepal where small and fragmented landholders dominate the farming system (Singha et al., 2019). Thus, Landsat data was selected over all other satellite images due to their high spatial resolution and cloud free data availability. The study area was selected for study as it had an appreciable amount of paddy rice agriculture and the availability of fine resolution satellite image required for the evaluation of the Landsat 8 based result. The algorithm, if effective, can be used in different regions within Nepal to assess and monitor rice area. This would be helpful for ensuring food security, change detection, biogeochemical nutrient cycling, methane emission, agricultural vulnerability and sustainability (Xiao et al., 2005).

2. Materials And Methods

2.1 Study Area

Sunsari and Morang are amongst the top most rice producing districts in Nepal in terms of both area and production (MOALD, 2018). In this study, we purposefully selected 12 local levels of the districts sunsari and morang. Namely: Itahari, Hansposha, Pakali, Aekamaba, Khanar, Bakaluru, Madhesa, Bhadgausinawar, Sundarpur, Dulari, Mrigauliya and Sisabanibadahara. The study area covers an area of 23,033 hectares. A part of the study area falls inside the SMIP (Sunsari Morang Irrigation Project) (NPCS, 2012).

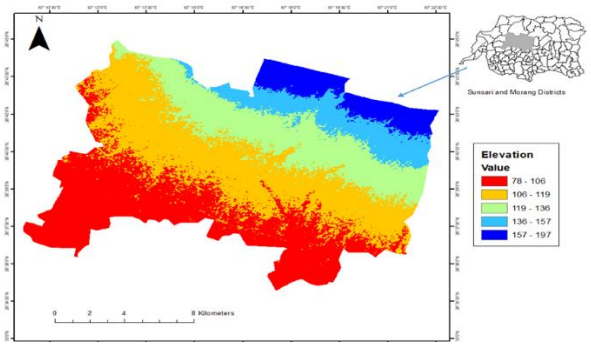

Figure 1: Digital Elevation Model (DEM) of the Study Area (https://earthexplorer.usgs.gov)

2.2 Data Collection

Multi-temporal imageries of 30-m spatial resolution Landsat OLI data were used for the study. High spatial resolution Landsat 8 data were purposely selected for the study over MODIS. Landsat 8 includes eleven bands. Nine series of Landsat 8 images were downloaded from the official website of the US geological survey (**https://earthexplorer.usgs.gov**) (Table 1). Images dating from 2013 to 2020 were used in the study.

Table 2: Details of Image Acquisition

Image Date	Sensor	Purpose
2013-09-08	OLI	Growth detection
2014-06-16	OLI	Flooding detection
2015-07-28	OLI	Flooding detection
2017-07-17	OLI	Flooding detection
2018-10-08	OLI	Growth detection
2018-12-27	OLI	Harvest detection
2019-06-05	OLI	Flooding detection
2019-11-28	OLI	Harvest detection
2020-06-07	OLI	Flooding detection

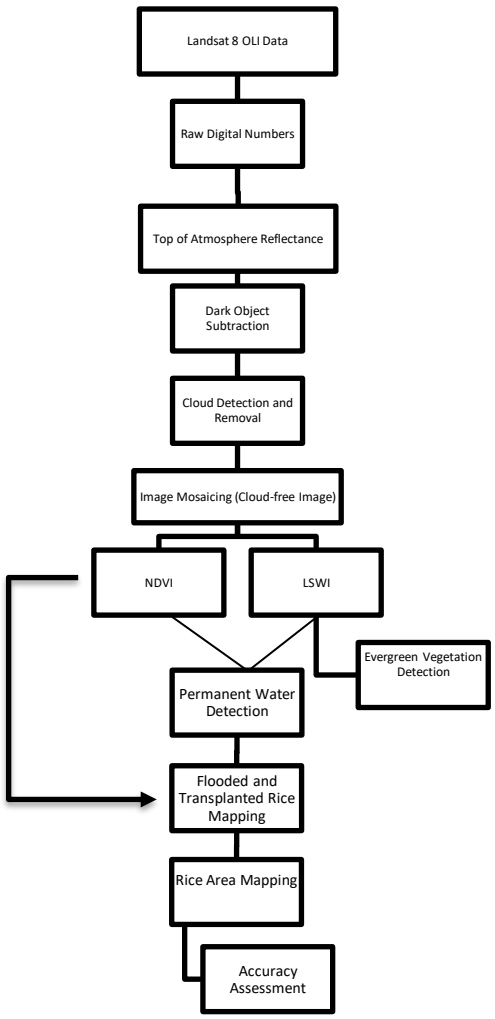

Figure 2: Overview of the Process involved in Mapping of flooding and paddy fields from Landsat 8 images at 30m resolution.

2.3 Pre-processing of Satellite Images

Radiometric correction was applied by converting the raw digital numbers into Top of atmosphere reflectance (TOA) using ENVI (version 5.3). Further, atmospheric correction was applied by identifying the darkest pixel value and subsequently subtracting this value from every pixel (Abdullah et al., 2019). Factors like Clouds, Evergreen vegetation, Water bodies and other vegetation cover can affect the detection of paddy area. Therefore, various masks were generated for cloud, Evergreen vegetation, Water bodies etc. to minimize their impacts using Arcgis (version 10.4).

2.4 Cloud Masking

Cloud mask was created with the help of Quality assessment band (BQA) for each tile. High LSWI of cloud pixels as compared to NDVI can cause

them to be identified as flooded pixels. Blue band was used to further remove the cloud pixels. Any pixels having blue band reflectance of ≥ 0.2 were also masked to be cloud pixels. Finally, all cloud observations were excluded from the study. Image mosaicking of images from different years of the same season was performed to obtain a single cloud free image for the month (Xiao et al., 2005; Li et al., 2004).

2.5 Evergreen coverage

Evergreen coverage can be separated into two parts: Evergreen forest and Shrubland. Evergreen forest has a consistently high NDVI value throughout the year while the agricultural lands have high NDVI for a little period at the end of the harvesting period. Therefore, pixels having NDVI value of more than 0.6 throughout the year are identified as evergreen forests. These were identified as evergreen forests. Unlike evergreen forest, shrub land has a comparatively low NDVI. LSWI of the agricultural land with the bare soil, like after harvesting or at ground preparation, is very low. According to available literatures, pixels having LSWI value not less than 0.15 throughout the year is considered to be evergreen vegetation (Xiao et al., 2005; S et al., 2018). Both the evergreen forest and shrubland were identified and removed from the study area to prevent misinterpretation.

2.6 Water Bodies

Water bodies can easily be misinterpreted as flooded pixels as both of them have high LSWI as compared to NDVI. During the initial stage of transplanting, the canopy cover is low due to which the reflectance from the flooded paddy field and water bodies cannot be separated. However, towards the end of the growing season, canopy cover increases. NDVI for the rice field slowly exceeds LSWI but remains the same in water bodies. Thus, LSWI > NDVI for all year round was used to detect the water bodies.

2.7 Calculation of vegetation indices

For each 16 day Landsat 8 data, we calculated NDVI and LSWI using the surface reflectance value from the Red (0.64-0.67 µm), NIR (0.85-0.88 µm) and SWIR 1 (1.57-1.65 µm) bands (Xiao et al., 2005):

$$NDVI = \frac{(NIR-RED)}{(NIR+RED)} \quad \text{eqn 1}$$

$$LSWI = \frac{NIR-SWIR1}{NIR+SWIR1} \quad \text{eqn 2}$$

NDVI corresponds to the leaf area index of the paddy fields while LSWI is sensitive to Soil and leaf water content(Zhang et al., 2015).

2.8 Identification of spatial distribution of rice

The algorithm of identifying rice areas is based on two indicators: LSWI (identifying the moisture level in the flooded rice area) and NDVI (identifying the growth of rice canopy and harvest). A unique characteristic of paddy is its flooding mechanism. Temporal dynamics of a paddy field can be separated into three stages: (1) flooding and transplanting; (2) Growth and pre-harvesting period with high vegetation cover and (3) Post harvest bareness. Detection of surface water and green vegetation requires is done by using the indices that use the spectral bands that are sensitive to both water and vegetation. Initial stage of the flooding, LSWI value is very high but decreases as the growth takes place. On the other hand, NDVI shows opposite behaviour.

During the transplanting stage, the rice field is a mixture of water and rice plant, and is covered by 2 to 15 cm of water. Due to the low canopy cover during the transplanting period, most of the reflectance is from soil and water. Thus, there is low NDVI and high LSWI. Pixels having LSWI>NDVI is used to identify flooded pixel. Considering the land fragmentation and ownership system in Nepal, Flooding and rice transplanting schedules may vary from one plot to another depending upon the farmer. This might be an obstacle for flooded pixel identification. Thus, to slightly ease the identification, the threshold to identify flooded pixels was changed to LSWI + 0.05≥NDVI.

As the tillering and growth starts, rice canopy quickly covers the flooded soil, decreasing the reflectance from water and soil and increasing the reflectance from green rice plants. Consequently, LSWI decreases and NDVI increases. LAI reaches peak within two months from transplant. Thus, the criteria that NDVI value reaches half of the maximum NDVI within two months after flooding was used to identify rice growth in flooded areas. An administrative boundary map at local level at the scale of 1:100000 was used to generate the summaries of rice area.

Rice map area might be underestimated or overestimated during the study due to various factors like fragmentation and sub-pixel proportion of rice area etc. Therefore, accuracy assessment of rice map needs to be done. However, budget constraints and human resource limitations, field survey for collection of ground truth points was not possible. Due to absence of pre-classified image and other ancillary data, an alternative approach to field survey, a fine resolution satellite image was used for accuracy assessment. In this study, 0.448m resolution image downloaded from digital globe open data program was used for validation of the map derived from 30m resolution Landsat image (Xiao et al., 2005).

3. Results And Discussion

Figure 3 shows the spatial distribution of paddy rice in the study area derived from Landsat 8 data. Paddy rice agriculture was prevalent throughout the study area except for the urbanized region in the middle. The rice area was found to be mostly concentrated in the south-western region and the region that lies under Sunsari-Morang irrigation project. This method uses the temporal profile analysis of the Landsat 8 derived vegetation indices and can be used to identify paddy rice fields at large scale. Rice fields are separated from other croplands due to the presence of water in rice fields during their initial phase of flooding and transplanting. Rice fields flooded with water are separated from other land use on the basis of their spectral reflectance.

Events like rainfall or irrigation can potentially alter the result predicted by the algorithm, leading to a situation where LSWI could approach or exceed NDVI. Wetlands are another region which could be identified as flooded rice areas by the algorithm. Previous land-use land cover map can be utilized to eliminate such areas for study. Cloud cover is an important constraint in monsoon season. Due to frequent cloud cover, a single cloud free image for the study area is difficult to obtain. Removal of the cloud and cloud shadow data was done and the cloud free "clean" data was mosaicked together to obtain single cloud free image (Li et al., 2004).

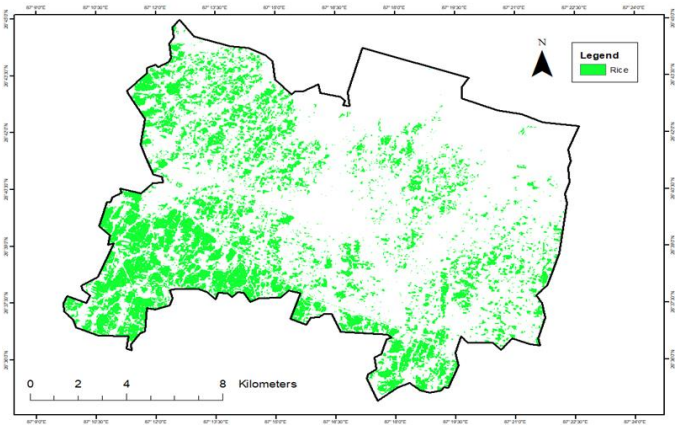

Figure 3: Spatial distribution of rice field in study area, as derived from the analysis of Landsat 8 data (at 30 m resolution)

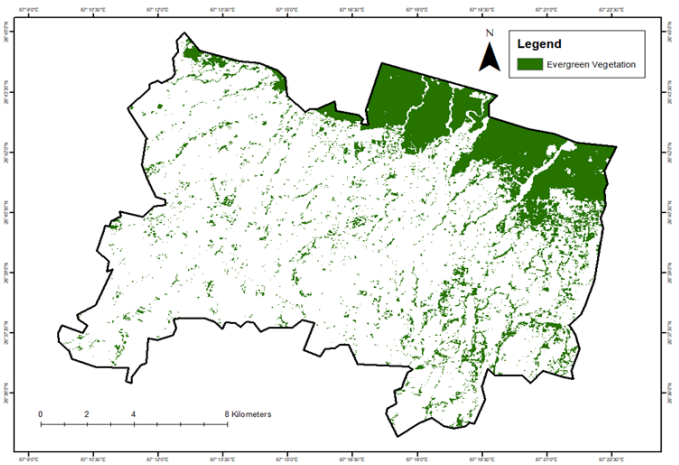

Figure 4: Spatial distribution of evergreen vegetation in study area, as derived from the analysis of Landsat 8 data (at 30 m resolution)

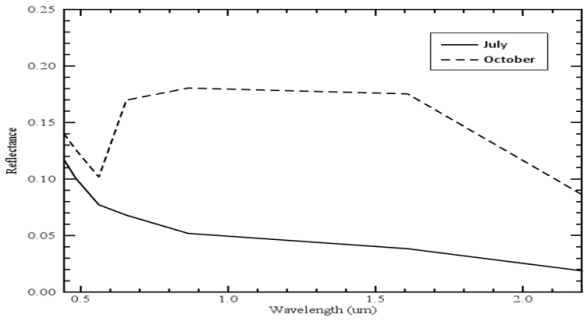

Figure 5: Spectral profile of Rice Area for the months of transplanting (July) and growth (October)

The above fig. 5 shows the spectral behaviour of the predicted rice field during the months of July and October. Due to flooding, water content in the rice field causes spectral reflectance to behave as above. Highest absorption can be seen at the SWIR region of the spectrum. Similarly, during the months of October, high vegetation content of the rice field causes the spectral reflectance to behave as such. There is high absorption in the red end of the spectrum.

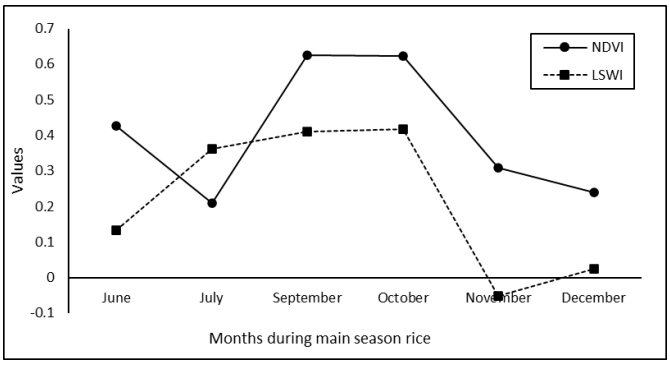

Figure 6: A comparison of average NDVI and LSWI indices of the predicted rice fields during different months in the rice growing season

Figure 6 explains the dynamics of NDVI and LSWI in the rice field. NDVI is always greater that LSWI all year round. However, during the flooding stage, the LSWI of the field approaches or exceeds the NDVI values. The algorithm identifies the pixels for which LSWI value approaches or exceeds NDVI. The accuracy assessment of this map was made using a high-resolution digital globe image downloaded from an open data program. During the process, a total of 79 field control points were taken in the study area, which included 49 control points for rice areas and 30 control points for non-rice areas. The overall accuracy of this method was found to be 79.746%. This result indicates that the given algorithm has potential to be applied using Landsat 8 data for monitoring rice fields on a periodic basis.

4. Conclusion

Accounting for about 42.5 percent of the total area and 51.6 percent of total food grain production, the importance of rice in Nepalese agricultural system is immense. Rice production has a significant role for ensuring food security amongst Nepalese people (Gadal et al., 2019). Monitoring rice area and production for conventional systems used is a tedious job. It requires a significant amount of time, budget, manpower and is not very accurate. Future of agriculture is changing rapidly with the advancement of technology. These technologies have facilitated the job which was previously considered tedious and labour intensive. Remote sensing is one of such technologies that is highly being used in developed countries for agricultural purpose. In this study, a simple algorithm using NDVI and LSWI obtained from Landsat 8 data was presented to assess the spatial distribution of rice area. The algorithm identified the rice areas with 79.746% of overall accuracy. These rice maps can be applied for assessing regional food security, water uses in rice production, methane emission assessment, spatial and temporal changes in paddy rice planting areas and yields for sustainable agricultural management practices.

Despite the stagnation of area and production of rice, the demand shows an increasing trend. Once a net exporter, Nepal currently faces rice shortage and is an importer of rice. This has led to a negative impact in the national economy. Sound planning for rice production is necessary for ensuring food security and reducing import of rice. Nepal could highly benefit from this technology of mapping rice. This technology can be used for measuring climate change impacts on rice like early-season drought, flood, temporal changes in rice areas. Water is one of the most important inputs for rice cultivation. Remote sensing could be used for monitoring water use in rice production. Sentinel-2 has higher resolution(i.e.10m) as compared to Landsat-8 images. Further, due to their high temporal resolution, there is a higher chance of obtaining cloud free images. Therefore, they could be used for further studies. This type of study can be conducted on other crops to obtain an algorithm for mapping the specific crop.

References

Abdullah, A.Y.M., Masrur, A., Gani Adnan, M.S., Al Baky, M.A., Hassan, Q.K., Dewan, A., 2019. Spatio-temporal patterns of land use/land cover change in the heterogeneous coastal region of Bangladesh between 1990 and 2017. Remote Sensing, 11 (7), Pp. 1–28. https://doi.org/10.3390/rs11070790.

Aburas, M.M., Abdullah, S.H., Ramli, M.F., Ashaari, Z.H., 2015. Measuring Land Cover Change in Seremban, Malaysia Using NDVI Index. International Conference on Environmental Forensics 2015 (iENFORCE2015), 30, Pp. 238-243.

Chandrasekar, K., Sesha, Sai, M.V.R., Roy, P.S., Dwevedi, R.S., 2010. Land Surface Water Index (LSWI) response to rainfall and NDVI using the MODIS vegetation index product. International Journal of Remote Sensing, 31 (15), Pp. 3987–4005. https://doi.org/10.1080/01431160802575653

Emara, S.R.S., Zeidan, B.A., Khadr, M., 2018. Modelling of Water Resources in the Nile Delta Using GIS and Remote Sensing, Faculty of Engineering, Tanta University.

Gadal, N., Shrestha, J., Poudel, M.N., Pokharel, B., 2019. A review on production status and growing environments of rice in Nepal and in the world. Archives of Agriculture and Environmental Science, 4 (1), Pp. 83–87. https://doi.org/10.26832/24566632.2019.0401013

Gumma, M.K., Gauchan, D., Nelson, A., Pandey, S., Rala, A., 2011. Temporal changes in rice-growing area and their impact on livelihood over a decade: A case study of Nepal. Agriculture, Ecosystems and Environment, 142 (3–4), Pp. 382–392. https://doi.org/10.1016/j.agee.2011.06.010

Ishtiaque, A., Shrestha, M., Chhetri, N., 2017. Rapid urban growth in the kathmandu valley, nepal: Monitoring land use land cover dynamics of a himalayan city with landsat imageries. Environments – MDPI, 4 (4), Pp. 1–16. https://doi.org/10.3390/environments4040072

Joshi, N., Dongol, R., 2018. Severity of climate induced drought and its impact on migration: a study of Ramechhap District, Nepal. Tropical Agricultural Research, 29 (2), Pp. 194. https://doi.org/10.4038/tar.v29i2.8289

Li, M., Liew, S.C., Kwoh, L.K., 2004. Automated Production of Cloud-Free and Cloud Shadow-Free Image Mosaics from Cloudy Satellite Imagery. Proceeding of 20th ISPRS Congress, Turkey, Pp. 523-530.

Meng, Y., Cao, B., Mao, P., Dong, C., Cao, X., Qi, L., Wang, M., Wu, Y., 2020. Tree species distribution change study in Mount Tai based on Landsat remote sensing image data. Forests, 11 (2), Pp. 1–14. https://doi.org/10.3390/f11020130

MoAD, 2015. Rice varietal mapping in Nepal: Implication for development and adoption, Crop Development Directorate, Nepal.

MOALD, 2018. Statistical Information on Nepalese Agriculture (2073/74). Publications of the Nepal in Data Portal, 73, Pp. 290.

Mosleh, M.K., Hassan, Q.K., Chowdhury, E.H., 2015. Application of remote sensors in mapping rice area and forecasting its production: A review. Sensors, 15 (1), Pp. 769–791. https://doi.org/10.3390/s150100769

Myneni, R.B., Hall, F.G., Sellers, P.J., Marshak, A.L., 1995. Interpretation of spectral vegetation indexes. IEEE Transactions on Geoscience and Remote Sensing, 33 (2), Pp. 481–486. https://doi.org/10.1109/36.377948

NPCS, 2012. Impact Evaluation of Sunsari-Morang Irrigation Project, Nepal.

Rahman, M.T., 2016. Detection of land use/land cover changes and urban sprawl in Al-Khobar, Saudi Arabia: An analysis of multi-temporal remote sensing data. ISPRS International Journal of Geo-Information, 5 (2). https://doi.org/10.3390/ijgi5020015

Sari, D.K., Ismullah, I.H., Sulasdi, W.N., Harto, A.B., 2010. Detecting rice phenology in paddy fields with complex cropping pattern using time series MODIS data: A case study of northern part of West Java-Indonesia. ITB Journal of Science, 42 A(2), Pp. 91–106. https://doi.org/10.5614/itbj.sci.2010.42.2.2

Singha, M., Dong, J., Zhang, G., Xiao, X., 2019. High resolution paddy rice maps in cloud-prone Bangladesh and Northeast India using Sentinel-1 data. Scientific Data, 6 (1), Pp. 1–10. https://doi.org/10.1038/s41597-019-0036-3

Thapa, C.D.B., 2017. Monitoring Urban Growth, Land Use and Land Cover Using Remote Sensing and Gis Techniques: A Case Study of Bhaktapur District, Nepal. IRACST – Engineering Science and Technology: An International Journal, 7 (1).

Xiao, X., Boles, S., Liu, J., Zhuang, D., Frolking, S., Li, C., Salas, W., Moore, B., 2005. Mapping paddy rice agriculture in southern China using multi-temporal MODIS images. Remote Sensing of Environment, 95 (4), Pp. 480–492. https://doi.org/10.1016/j.rse.2004.12.009

Xiao, X., He, L., Salas, W., Li, C., Moore, I., Zhao, R., Frolking, S., Boles, S., 2002. Quantitative relationships between field-measured leaf area index and vegetation index derived from VEGETATION images for paddy rice fields. International Journal of Remote Sensing, 23 (18), Pp. 3595–3604. https://doi.org/10.1080/01431160110115799

Yadav, N.K., Qamer, F., Matin, M., 2017. Mapping major crops using Sentinel Images for Nepal, SARI Workshop, Delhi.

Zarkesh, M.K., Safaval, P.A., 2018. Mapping the Spatial Distribution of Rice Fields in Southern Coast of Caspian Sea Using Landsat 8 Time-series Images. Journal of Geography and Natural Disasters, 08 (01), Pp. 1–8. https://doi.org/10.4172/2167-0587.1000215

Zhang, G., Xiao, X., Dong, J., Kou, W., Jin, C., Qin, Y., Zhou, Y., Wang, J., Menarguez, M. A., Biradar, C., 2015. Mapping paddy rice planting areas through time series analysis of MODIS land surface temperature and vegetation index data. ISPRS Journal of Photogrammetry and Remote Sensing. 106, Pp. 157–171. https://doi.org/10.1016/j.isprsjprs.2015.05.011.